Key Engineering Materials
ISSN: 1662-9795, Vol. 755, pp 170-180
doi:10.4028/www.scientific.net/KEM.755.170

Submitted: 2017-04-20
Revised: 2017-05-19
Accepted: 2017-05-24
Online: 2017-09-14

Pushover Analysis Based on Equivalent Diagonal Springs for the Assessment of the Seismic Safety of Post-and-Beam Timber Buildings Braced with Nailed Shear Walls

Natalino Gattesco[1,a] and Ingrid Boem[1,b*]

[1]Department of Engineering and Architecture, University of Trieste, p.le Europa 1, Trieste, Italy

[a]gattesco@units.it, [b]boem@dicar.units.it

Keywords: Timber structures, Post-and-beam system, Timber shear-walls, Seismic behavior, Numerical simulations, Pushover analysis

Abstract. A method for a simplified modeling of post-and-beam timber buildings braced with nailed shear walls, useful for seismic design purposes, is presented and discussed in the paper. This strategy is based on the schematization of the vertical diaphragms through equivalent diagonal springs with elastic-plastic behavior and allows the assessment of the resisting ground acceleration by performing nonlinear static analysis; the Capacity Spectrum method based on equivalent viscous damping was applied. This nonlinear procedure constitutes a reliable and simple alternative to the linear static analysis using the behavior factor q. The procedures to determine the characteristics of the equivalent elements (stiffness and load-carrying capacity) are based on analytical evaluations, starting from the actual characteristic of shear walls. A comparison between the results of numerical simulation based of more refined and complex models, previously presented by the authors, and this time-reducing, simplified analysis proved the good reliability of the method.

Introduction

A great attention to the design of timber constructions in seismic prone areas was devoted in the last decades so to guarantee adequate structural safety of buildings subjected to earthquake excitation through simple design methods. The paper focuses on the behavior of ‘‘Post-and-beam’’ timber structures, consisting in a main frame of continuous floor-to-roof posts, connected to the foundation through steel devices, and horizontal beams, pin connected to the vertical elements. The vertical bracing system is commonly provided by timber shear walls [1]-[2], made with wood-based sheathings nailed to a timber light frame, connected to the main structure. The good seismic performances, which can be attained by these structures, are for the most related to the dissipative capacities (cyclic yielding) of the nailed connections of the shear walls (dissipative zones) [3].

According to [3], in earthquake-resistant timber buildings designed in agreement with the concept of dissipative structural behavior, the seismic design may be done on the basis of a linear static analysis of the structure, taking implicitly into account its dissipative capacity by using a design response spectrum equal to the elastic one reduced by the behavior factor q. Recently, the authors performed some refined numerical analysis on case-study buildings [4], so to assess the actual values range for the behavior factor to be used for a reliable seismic design based on linear static analysis. The study concerned non-linear static analysis on a detailed numerical model, in which the different connections were explicitly modeled, calibrating their nonlinear behavior through experimental results. From the study emerged that the maximum value of the behavior factor allowed in Eurocode 8 for “timber structures made of nailed wall panels with nailed diaphragms, connected with nails and bolts” (q = 5) overestimates the actual one for the considered structural typology. Therefore, a lower value of the behavior factor (close to 3) has to be assumed.

As an alternative to this approach, a simplified nonlinear static analysis is proposed in this paper for the seismic design of post-and-beam timber buildings. It consists in modeling the vertical diaphragms by means of equivalent, elastic-plastic diagonal springs accounting for the global nonlinear behavior of the different shear walls. The evaluation of both the elastic stiffness and shear

resistance of the equivalent elements are based on analytical relationships, which are discussed in the paper; the ultimate allowable drift of the shear walls is based on experimental and numerical evidences. The simplified method is applied, at first, for the simulation of the behavior of some shear walls with and without openings, tested experimentally by the authors [5] and, then, of the post-and-beam timber buildings already analyzed through the refined modeling [4]. A comparison of the results with those obtained from the refined numerical model in terms of capacity curves and resisting ground acceleration permits to assess the reliability of this simplified method, which represents an effective and rapid alternative to linear static analysis for ensuring the timber building seismic safety.

Method

The simplified method proposed for nonlinear analysis of post-and beam timber buildings braced with nailed timber shear walls consists in modeling posts and beams by means of mono-dimensional pinned elements with linear elastic material. The global horizontal stiffness is provided by the shear walls, that are modelled through two nonlinear axial springs arranged along the diagonals of the main frames. In particular, an elastic-plastic, symmetric behavior was considered. The characteristics of the spring, in terms of both stiffness and resistance, were evaluated analytically. The assumed ultimate allowable drift was based on experimental and numerical evidences.

Stiffness. By applying the principle of virtual work and through the equivalence of the actual shear wall deformability (δ_{tot}) and that of the simplified model (δ'_{tot}), it is possible to deduce the stiffness K_{eq} of the equivalent springs from the actual shear wall stiffness K_{tot} (Fig. 1) as

$$K_{eq} = K_{tot} \frac{H^2 + B^2}{2B^2}, \tag{1}$$

where B and H are the width and the height of the shear wall, respectively.

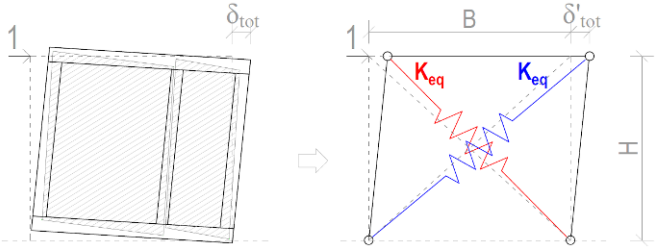

Fig. 1 Modeling of a shear wall with equivalent diagonal springs

The elastic stiffness K_{tot} of a shear wall composed by n_w segments (sheathing panels arranged alongside) can be evaluated through Eq. 2, considering the sum of the different contributions to the global displacement of the top of the wall (δ_{tot}) induced by a unitary horizontal force at the top (Fig. 2). These contributions are due to the flexural displacement of the timber frame as a cantilever, δ_b (Eq. 3), the rotation at the base of the wall, δ_c (Eq. 4), and the equivalent displacement of the n_w wall segments acting separately (in parallel), δ_{seg}:

$$K_{tot} = \frac{1}{\delta_{tot}} = \frac{1}{\delta_b + \delta_c + \delta_{seg}} \quad \text{with} \quad \frac{1}{\delta_{seg}} = \sum_{i=1}^{n_w} \frac{1}{\delta_i} = \sum_{i=1}^{n_w} \frac{1}{\delta_{s,i} + \delta_{sf,i} + \delta_{ns,i}}, \tag{2}$$

where $\delta_{s,i}$ (Eq. 5) is due to the shear deformation of the sheathing, $\delta_{sf,i}$ (Eq. 6) is caused by the horizontal slip of shear connectors at the base of the segment and $\delta_{ns,i}$ (Eq. 7) is due to the slip in the perimeter nail connections between the sheathing and the frame.

$$\delta_b = \frac{2H^3}{3E_0AB^2} \tag{3}$$

$$\delta_c = (\delta_{vc} + \delta_{vt})\frac{H}{B} = \left(\frac{h_j}{E_{90}A_{eq}} + \frac{\delta_h}{n_h}\right)\frac{H^2}{B^2} \tag{4}$$

$$\delta_{s,i} = \frac{H}{GB_i\, t} \tag{5}$$

$$\delta_{sf,i} = \frac{1}{n_{sf,i}K_{sf,i}} \tag{6}$$

$$\delta_{ns,i} = \delta_{nsx,i} + \delta_{nsy,i} = \frac{p}{K_{pf}B_i n_p}2\left(1 + \frac{H}{B_i}\right) \tag{7}$$

A, E_0 cross section and Young modulus parallel to grain of studs;
δ_{vc}, δ_{vt} vertical displacements at the two opposite ends of the shear wall due to the compression of the base timber joist and to the deformation of the hold-down connections subjected to tension, respectively;
h_j depth of the cross section of the base joist;
E_{90} Young modulus perpendicular to grain of the base timber joist;
A_{eq} stud equivalent cross section;
δ_h vertical displacement of a single hold-down connection stressed by a unitary vertical force;
n_h number of hold-down subjected to tension;
G sheathing shear modulus;
B_i width of the i-th segment of the shear wall;
t global thickness of the sheathing;
$K_{sf,i}$ stiffness of the single base shear connection;
$n_{sf,i}$ number of base shear connections in the i-th segment;
$\delta_{nsx,i}$ horizontal displacement due to the deformation of nails between sheathing and the joists;
$\delta_{nsy,i}$ horizontal displacement due to the deformation of nails between sheathing and the studs;
p nail spacing;
$K_{p\text{-}f}$ slip modulus of the single timber-to-timber nail;
n_p = 2 for sheets on both sides, 1 otherwise.

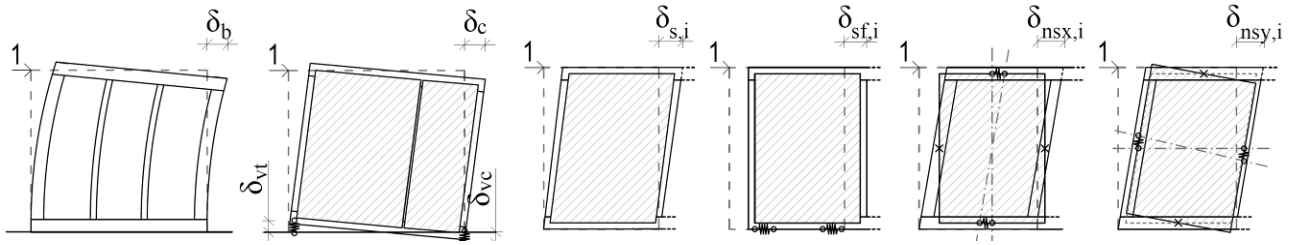

Fig. 2 Contributions to the shear wall in-plane deformability: (a) flexural deflection of the timber frame, (b) rotation at the base of the wall, (c) slip of base shear connectors, (d) shear deformation of sheathing, deformation of nails (e) between sheathing and the joists and (e) between sheathing and the studs

The deformability of the single hold down connection, δ_h, can be assessed experimentally, by means of characterization tests [5]; however the authors developed an analytical relationship, based of different contributions:

$$\delta_h = \delta_{h1} + \delta_{h2} + \delta_{h3} + \delta_{h4} + \delta_{h5}, \tag{8}$$

which accounts for the vertical displacements due to the nail slip (δ_{h1}), the out-of-plane flexural displacement of the hold-down (δ_{h2}), the flexural displacement of the hold-down base (δ_{h3}), negligible in the presence of a base thick prismatic washer, and the axial deformation of both the vertical plate of the hold-down (δ_{h4}) and the anchor bolt (δ_{h5}).

The various displacement contributions may be evaluated through the following relationships:

$$\delta_{h1} = \frac{1}{n_{n,h} K_{ser,h1}} \tag{9}$$

$$\delta_{h2} = \frac{l_7^2}{E_s l_5 s^3} \quad \frac{l_2 \xi^3}{(1 - \xi + \xi^2/3)} \qquad \text{with} \qquad \xi = \frac{l_3}{l_2} \tag{10}$$

$$\delta_{h3} = \frac{1}{4 E_s l_5 s^3} \quad \frac{(l_5 - \Phi_k)}{2} \left[3 l_5^2 - (l_5 - \Phi_k)^2 \right] \frac{1}{n_s} \tag{11}$$

$$\delta_{h4} = \frac{L_{h4}}{E_s l_5 s} \qquad \text{with} \qquad L_{h4} = \frac{1}{2}(l_1 - l_2) + l_4 + \frac{(l_2 - l_4)}{2} \tag{12}$$

$$\delta_{h5} = \frac{L_{h5}}{E_s A_{h5}} \tag{13}$$

$n_{n,h}$ number of nails in the hold down;
$K_{ser,h1}$ slip modulus per shear plane per fastener (if a wooden-based panel is interposed between the hold-down and the timber studs, it is necessary to consider both the slip modulus of the steel-to-panel connection and that of the panel-to-frame, by summing them in parallel);
E_s Young modulus of the steel;
l_2 distance of the first nail row from the base;
l_3 distance of the first nail row from the ribs weld;
l_4 the distance of the first nail row from ribs;
l_5 hold-down width;
l_7 distance between the axis of the threaded rod and the vertical plate of the hold down;
s hold-down thickness;
ϕ_k hole diameter at hold-down base;
n_s number of overlapping steel sheets forming the hold-down base;
L_{h4} equivalent length of the hold-down vertical plate;
L_{h5}, A_{h5} equivalent length and the net cross section of the bolt.

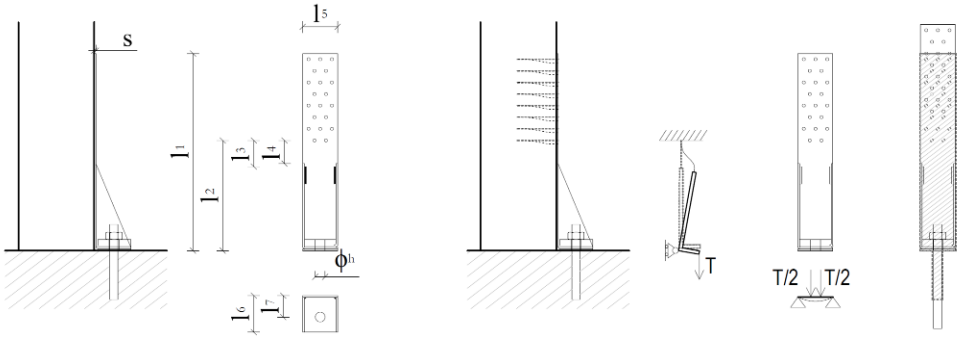

(a) (b) (c) (d) (e)

Fig. 3 Schematization of hold-down geometry (a) and contributions to the hold-down axial deformability: (b) nail slip, (c) out-of-plane flexural displacement of the hold-down, (d) flexural displacement of the hold-down base and (e) axial deformation of both the vertical plate of the hold-down and the anchor bolt

As already evidenced by the authors [7], the described analytical approach, developed for shear walls without openings and based on the global wall rotation at the base (Fig. 2b), provides reliable results also in case of small openings; diversely, for large openings, it resulted more realistic to consider the independent rotation of the different wall segments. The additional contribution of the sheathing panels $\delta_{i,op}$, over and below the opening (suffix ‘ and “, respectively) of the perforated segment should also be considered for an appropriate evaluation, especially in this latter case:

$$\delta_{i,op} = \delta_{s,i} + \delta_{sf,i} + \delta_{ns,i} = \frac{1}{\frac{1}{\delta'_{s,i}} + \frac{1}{\delta''_{s,i}}} + \delta_{sf,i} + \frac{1}{\frac{1}{\delta'_{ns,i}} + \frac{1}{\delta''_{ns,i}}}, \quad (14)$$

$$\text{with } \frac{1}{\delta^{j}_{s,i}} = \frac{h^{j} G B_i t}{H^2} \quad \text{and} \quad \frac{1}{\delta^{j}_{ns,i}} = \frac{2 p H^2}{K_{p-f} h^{j} B_i n_P} \left(\frac{1}{h^{j}} + \frac{1}{B_i} \right).$$

Strength. The equivalent springs resistance, F_{eq}, can be derived from the actual, lateral resistance of the shear wall, F_v:

$$F_{eq} = F_v \frac{\sqrt{H^2 + B^2}}{2B}. \quad (15)$$

For the calculation of the shear walls lateral resistance, F_v, the simplified model proposed in Eurocode 5 [6] may be adopted. This approach is based on the assumption of pure shear flow along the perimeter of the sheathing: the force on each fastener is considered at most equal to the plastic capacity of the fastener f_{nail} and the force distribution parallel with the framing members. By adopting such a simplified method, a 20% increased equivalent resistance should be considered for the fasteners along the edges, so to predict the actual lateral load carrying capacity (and displacement capacity) of the shear wall (as proved also in [4] by the authors).

When a segmented shear-wall is considered (n_w sheathing panels arranged alongside), its global capacity is estimated as the sum of the resistances of the different segments $F_{v,i}$:

$$F_v = \sum_{i=1}^{n} F_{v,i} \quad \text{with} \quad F_{v,i} = \frac{1.2 \cdot f_{nail} \cdot B_i \cdot c_i \cdot n_p}{p}, \quad (16)$$

being p the nails spacing, n_p =2 for sheathing applied at both sides, n_p =1 otherwise, and shape factor $c_i = 1$ if $B_i > H/2$ or $c_i = 2B_i/H$ otherwise.

In perforated segments, as evidenced by the authors [7], the resistance contribution of the nailed sheathings below the opening can be considered through the relationship:

$$F_{v,i} = \frac{1.2 \cdot f_{nail} \cdot h_i \cdot c_i \cdot n_p}{p}, \quad (17)$$

where h_i is the sheathing height and the shape factor c_i is = 1 if $B_i > h_i/2$ or = $2B_i/h_i$ otherwise.

Ultimate displacement. The ultimate displacement of the diagonal, $s_{u,eq}$, is calculated from the ultimate horizontal displacement of the shear wall $s_{u,tot}$, according to the relationship:

$$s_{u,eq} = s_{u,tot} \frac{B}{\sqrt{H^2 + B^2}}. \quad (18)$$

By analyzing the actual behavior of several shear walls with different characteristics, subjected to horizontal cyclic loading ([5], [8]-[10]), it was observed that the value of $s_{u,tot}$ are comparable and ranged approximately between 1.5% to 2.0 % of the wall height. Thus, it is reasonable to assume, prudentially, a maximum drift of 1.5% as reference for the considered vertical diaphragms.

Validation of the Method

To clarify and validate the procedure described in the previous section, some cases were analyzed with the simplified pushover analysis based on equivalent diagonal springs. In particular, six timber shears walls and three post-and-beam timber structures were investigated.

Single timber shear walls. Six timber shear walls (PLS3-8), already subjected in the recent past to in-plane quasi-static cyclic tests ([5], [11]), were modelled by means of the equivalent diagonal springs method and the results were then compared with the experimental ones in terms of capacity curve.

The main characteristics of the sample PLS3 are resumed in Fig. 4a; PLS4 differed from PLS3 for the absence of the opening and of the hold-down connections in the intermediate segment and for doubled anchor bolts at the base (3 in segment at left, 2 in the intermediate one and 1 in that at right). PLS6 had the same characteristics of the left segment of PLS4, with couples of hold-down WHT340 applied at ends. A doubled nail spacing was considered in PLS5, in respect to PLS6; moreover the WHT340 connections were replaced by WHT620 hold-downs (52 ring nails Φ4/60, δ_h = 0.2117 mm/kN) and the 3 M16 anchor bolts with 6 M20. Fig. 4b summarizes the main characteristics of the sample PLS8; thicker cross section for both the main frame (160x200 mm^2 studs, 200x120 mm^2 joists) and the sheathing panels (t = 40 mm) were considered for PLS7.

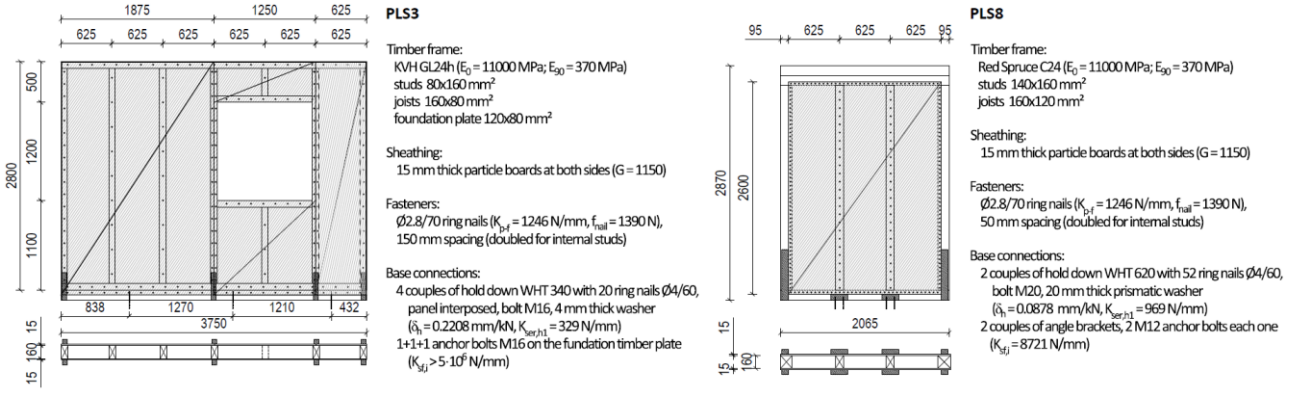

(a) (b)

Fig. 4 Main characteristics of shear walls (a) PLS3 and (b) PLS8

It is observed that the slip modulus K_{p-f} and the plastic capacity f_{nail} of the single timber-to-timber nail were determined starting from the actual capacity curve of the fastener [5] by adopting an idealized elastic-plastic relationship, assuming as for K_{p-f} the secant value to the curve in correspondence to the force value equal to 0.6 of the peak one, f_{max}. The maximum displacement capacity was evaluated in correspondence of a 15% reduction of f_{max} in the post peak branch; the yield force f_{nail} was determined in a way that the areas under the actual and the idealized force-displacement curves resulted equal.

The values of the different contributions for the evaluation of the equivalent stiffness K_{eq}, resistance F_{eq} and ultimate displacement $s_{u,eq}$ are reported in Table 1.

Table 1 Analytical evaluation on shear walls

		PLS3	PLS4	PLS5	PLS6	PLS7	PLS8
$\delta_{s,i}$	[mm/kN]	0.0433 0.3636/0.1653 0.1299	0.0433 0.0649 0.1299	0.0433	0.0433	0.0296	0.0403
$\delta_{sf,i}$	[mm/kN]	<10^{-5} 0.1601	<10^{-5} 0.1601	<10^{-5}	<10^{-5}	0.0287	0.0287
$\delta_{ns,i}$	[mm/kN]	4.2283/1.1731 1.0555	0.3120 1.0555	0.0800	0.1601	0.0768	0.0464
δ_i	[mm/kN]	0.2034 1.0320 1.1854	0.2034 0.3770 1.1854	0.1233	0.2034	0.1351	0.1154
δ_{seg}	[mm/kN]	0.1486	0.1189	0.1233	0.2034	0.1351	0.1154
δ_{vc}	[mm/kN]	0.0126	0.0126	0.0252	0.0252	0.0138	0.0201
δ_h	[mm/kN]	0.2208	0.2208	0.2117	0.2208	0.0878	0.0878
δ_{vt}	[mm/kN]	0.0824	0.0824	0.1580	0.1649	0.0599	0.0610
δ_b	[mm/kN]	<10^{-5}	<10^{-5}	<10^{-5}	<10^{-5}	<10^{-5}	<10^{-5}

δ_c	[mm/kN]	0.0710	0.0710	0.2737	0.2839	0.1004	0.1128
δ_{tot}	[mm/kN]	0.2196	0.1898	0.3970	0.4873	0.2356	0.2282
K_{tot}	[kN/mm]	4.55	5.27	2.52	2.05	4.25	4.38
K_{eq}	**[kN/mm]**	**3.55**	**4.10**	**4.07**	**3.31**	**6.07**	**6.42**
F_i	[kN]	41.70 24.46 6.21	41.70 24.82 6.21	83.40	41.70	140.45	137.78
F_v	[kN]	72.37	72.73	83.40	41.70	140.45	137.78
F_{eq}	**[kN]**	**45.16**	**45.38**	**74.94**	**37.47**	**118.74**	**117.95**
$s_{u,tot}$	[mm]	42.00	42.00	42.00	42.00	43.05	43.05
$s_{u,eq}$	**[mm]**	**33.65**	**33.65**	**23.37**	**23.37**	**25.46**	**25.14**

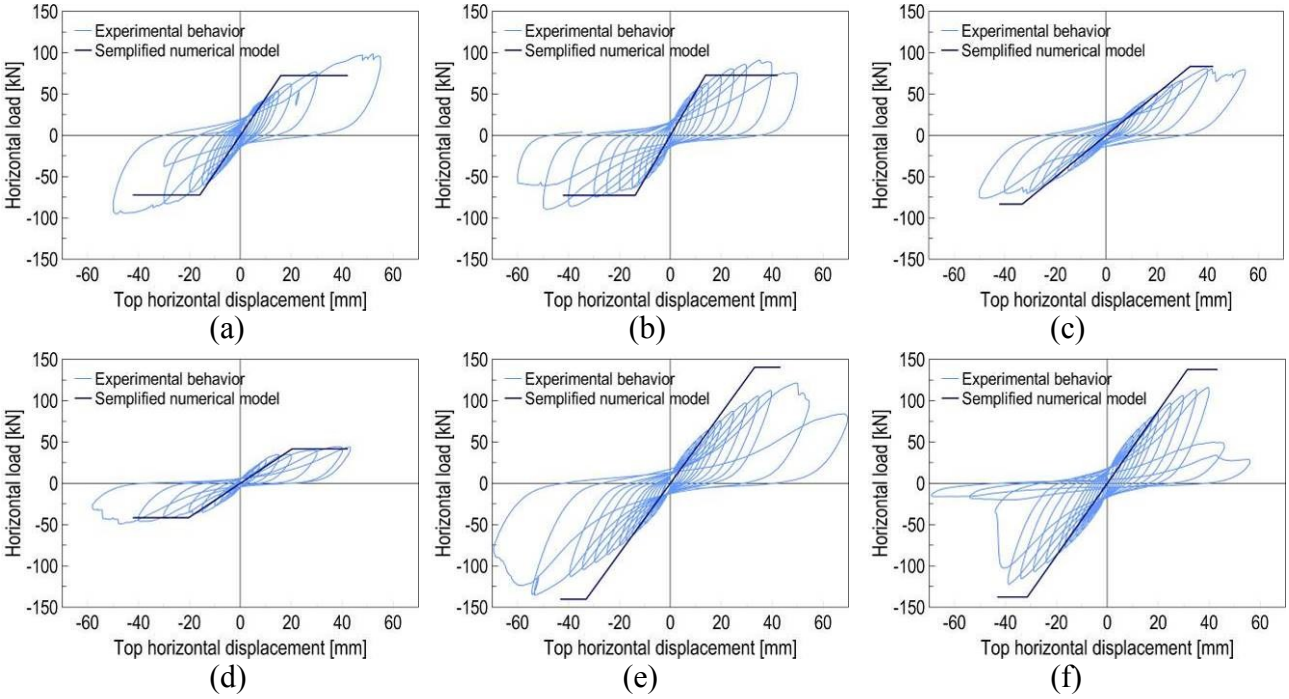

Fig. 5 Comparison between the numerical results, deduced from the simplified nonlinear analysis based on equivalent diagonal springs, and the experimental performances of the shear walls: (a) PLS3, (b) PLS4, (c) PLS5, (d) PLS6, (e) PLS7 and (f) PLS8

It is observed that, for the evaluation of the stiffness of the perforated shear wall, PLS3, the global wall rotation at the base was assumed and the additional contribution of the sheathing panels over and below the opening were considered, according to Eq. 14. Moreover, in the resistance evaluation, the contribution of the nailed sheathing below the opening was considered (Eq. 17).

The results (Fig. 5) generally evidenced a good agreement of the simplified elastic-plastic graph with the experimental backbone curve.

Post-and-beam timber buildings. The simplified modeling method was then applied for the numerical simulation of the seismic behavior of post-and-beam timber structures braced by nailed shear walls. In particular, the three buildings already analyzed by the authors [4] were considered (Fig. 6). The seismic-resistant system of the structures was composed by shear walls connected to the posts and to the beams at each storey, as schematized in Fig. 7a. Couples of hold-down were applied at the base of the posts and of each stud close to openings. Moreover, a couple of angle brackets was placed on the base joist of the shear walls, in correspondence of each segment. According to [3], hold-down and angle brackets connections were over-dimensioned so to force the development of cyclic yielding only in the nails of the sheathing. The main characteristics of the structure are resumed in Table 2.

In [4][1], the main frame was modelled by vertical continuous elements (posts), with horizontal elements (main and secondary beams) and vertical studs pinned (Fig. 7b); a linear-elastic behaviour for all wooden components was considered. A rigid floor diaphragm was assumed for each storey

level. Two-dimensional elements represented the wood-based sheets, which were connected to the timber frame by means of mono-dimensional nonlinear springs, acting only in the direction of the timber element to which they are connected. Mono-dimensional non-linear springs were employed to model also, the deformability of the stud–joist, the hold down connections and the angle brackets connections. The non-linear behavior of the different connections was derived from experimental tests. By performing non-linear static analysis (pushover) on this refined numerical model, it was possible to derive the capacity curves of the structure, which represents the relation between the base shear force and the displacement of the control node, taken as the centroid of the roof floor of the building.

In the present study, the building model was simplified (Fig. 7c): equivalent diagonal springs connecting the main frame nodes were introduced to represent the shear wall diaphragm action. It is worth note that the stiffness of the equivalent elements at the ground floor accounted also for the hold-down deformability. Diversely, the springs accounting for the slip of base shear connectors were condensed at the base of the posts, for simplicity.

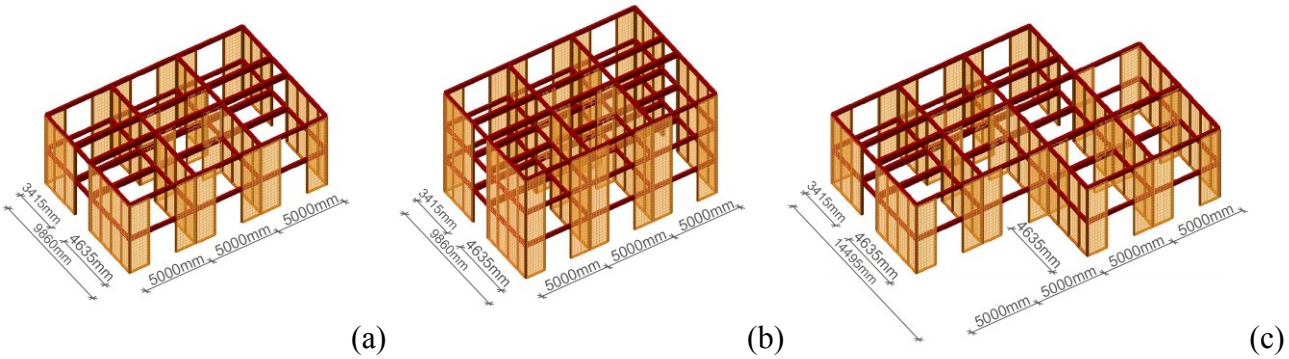

(a) (b) (c)

Fig. 6 Main dimensional characteristics of the analyzed buildings: (a) two storey regular 2R, (b) three storey regular 3R and (c) two storey non-regular in plan 2I [1].

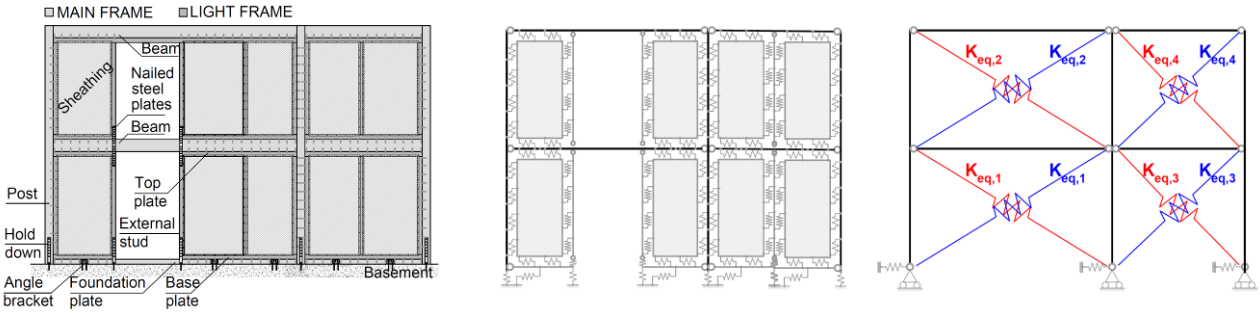

(a) (b) (c)

Fig. 7 Schematization of (a) the considered structural type for post-and-beam timber buildings, (b) the refined numerical model adopted in [4] and (c) the simplified numerical model based on equivalent diagonal springs

Table 2 Main characteristics of the considered post-and-beam timber structures

Building characteristics	
Inter-storey height	3000 mm
Timber	Red spruce C24
Intermediate storey mass (seismic)	490 kg/m^2
Roof mass (seismic)	210 kg/m^2
Main frame	
Posts cross section	160x160 mm^2
Central beams cross section	200x480 mm^2
Edge and secondary beams cross sec.	160x320 mm^2
Elastic stif. of an hold down	14000 N/mm
Elastic stif. of an angle bracket	16000 N/mm

Timber shear walls	
Light frame elements cross section	80x135 mm^2
Sheathing panels	OSB, on one side
Sheathing height	2790 mm
Sheathing width, X direction	1445 mm
Sheathing width, Y direction	975/1220 mm
Sheathing thickness	25 mm
Sheathing-light frame connection	ϕ2.8 ring nails
Plastic capacity of the single nail	1.2*1081 N
Elastic stiffness of the single nail	1.2*692 N/mm
Nail edge distance	20 mm

The stiffness and strength characteristics of the equivalent elements were calculated according to the analytical procedure described and are reported for the different shear wall configurations in Table 3. In particular, three different segmented shear walls were considered:

- "X": 5000 mm width shear wall composed by two 1445 mm width segments with a full-height opening in between.
- "Y_a": 4635 mm width shear wall composed by three 1220 mm width segments and one 975 mm width segment;
- "Y_b": 3415 mm width shear wall composed by two 1220 mm width segments and one 975 mm width segment;

It is observed that the nail spacing (reported in Table 3) was designed in [4] by performing a preliminary elastic analysis (with q=3); the maximum shear forces acting in each floor for the different sheet widths was considered. The connection between the light frame and the main frame was considered rigid, assuming the absence of tolerances between the light and the main frame.

Table 3 Nail spacing p and equivalent stiffness K_{eq} and resistance F_{eq} for the different building configurations considered

ID	Floor	p [mm]			K_{eq} [kN/mm]			F_{eq} [kN]		
		B_i=1445mm	B_i=1220mm	B_i=975mm	X	Y_a	Y_b	X	Y_a	Y_b
2R	1st	118	138	95	1.99	2.64	2.38	18.53	23.81	19.76
	2nd	240	280	169	1.09	1.52	1.42	9.11	12.13	10.17
3R	1st	107	101	89	2.16	3.26	2.87	20.43	30.85	25.13
	2nd	121	104	97	2.02	3.38	3.03	18.07	29.64	24.05
	3nd	228	218	222	1.15	1.72	1.54	9.63	13.92	11.23
2I	1st	118	112	88	1.99	3.06	2.72	18.53	28.48	23.40
	2nd	235	205	161	1.11	1.91	1.74	9.30	15.56	12.78

Nonlinear static analyses were performed considering, for both the building main directions, two different distributions of the lateral loads, as suggested in Eurocode 8: a modal pattern (S), proportional to the fundamental mode shape, and a uniform pattern (M), with lateral forces proportional to mass regardless of elevation (uniform response acceleration).

According to the Capacity Spectrum Method based on equivalent viscous damping [12]-[14], described in detail in [4], the maximum ground acceleration $a_{g,max}$ that may be supported by the structure can be evaluated by means of Eq. 19, by intersecting the ultimate displacement of the capacity curve of the equivalent single degree of freedom system (SDOF) system d*u with the design response spectrum for the effective current period T^*_{eff} and damping η_{eff}:

$$a_{g,max} = \frac{4\pi^2 d^*_u}{S\eta_{eff}\ 2.5\ T_C\ T^*_{eff}} \quad \text{if} \quad T_C \le T^*_{eff} \le T_D, \tag{19}$$

where S is the soil factor, T^*_{eff} the effective period of the idealized equivalent SDOF associated to d^*_u and periods T_C and T_D define, respectively, the end of the constant spectral acceleration branch and the beginning of the constant displacement response. In [4] the authors evidenced that the effective damping correction factor η_{eff}, for the considered structural type, ranges from about 0.63 to 0.71; thus, an average value of 0.67 was herein assumed in the calculations.

The capacity curves of the structures deduced from the simplified pushover analysis were evaluated and compared to that derived from the previous pushover analysis obtained with the refined model (Fig. 8a-b); very good accordance of the results emerged, proving the reliability of the simplified model. The comparison in terms of a_g, reported in Fig. 8c, evidenced that the values deduced from the simplified model are generally on the safe side.

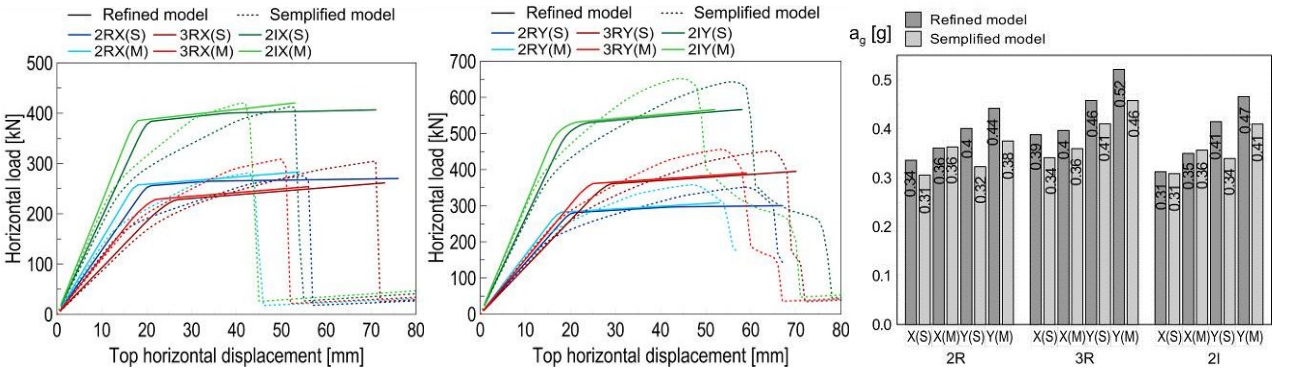

(a) (b) (c)

Fig. 8 Comparison between the post-and-beam timber structures: capacity curves derived from simplified (solid lines) and detailed (dotted lines) numerical simulation in the (a) X and (b) Y direction and (c) resisting ground accelerations a_g

Conclusion

The paper presented a simplified modeling method for the seismic design of post-and-beam timber buildings braced with nailed shear walls, based on nonlinear static analysis. The method consists in the simplified modeling of the vertical diaphragms by means of equivalent diagonal springs accounting for the nonlinear in-plane behavior of the shear walls. An elastic-plastic behavior was assumed for the springs: the evaluations of both the stiffness and resistance were based on analytical relationships; the ultimate displacement was based on experimental evidences.

The simplified method was applied, at first, for the simulation of the behavior of some shear walls tested experimentally and, then, to study whole post-and-beam timber buildings, recently analyzed by the authors through refined nonlinear models.

The comparison of the results proved the good reliability of the simplified modeling method, which represents an effective and rapid alternative to linear static analysis based on *q*-factor for ensuring the seismic safety of post-and-beam timber buildings.

Acknowledgments

The financial support of "Reluis 2016" is gratefully acknowledged.

References

[1] A. Buchanan, B. Deam, M. Fragiacomo, S. Pampanin, A. Palerm, Multi-Storey Prestressed Timber Buildings in New Zealand. Structural Engineering International 18, 2 (2008) 166-173.

[2] G. Parida, M. Fragiacomo, H. Johnsson, Prefabricated timber walls anchored with glued-in rod connections: racking tests and preliminary design, Eur. J. Wood Prod. 71, 5 (2013).

[3] EN 1998-1:2004, Eurocode 8: Design of structures for earthquake resistance - Part 1: General rules, seismic actions and rules for buildings, CEN, Bruxelles, 2004.

[4] N. Gattesco, I. Boem, Seismic performances and behavior factor of post-and-beam timber buildings braced with nailed shear walls, Engineering Structures 100 (2015) 674–685.

[5] N. Gattesco, I. Boem, Stress distribution among sheathing-to-frame nails of timber shear walls related to different base connections: Experimental tests and numerical modelling, Construction and Building Materials 122 (2016) 149-162.

[6] EN 1995-1-1:2004/A2:2014, Eurocode 5: Design of timber structures - Part 1-1: General - Common rules and rules for buildings, CEN, Brussels, 2014.

[7] N. Gattesco, I. Boem, Finite element models for perfortared timber shera walls, Personal communication (2017).

[8] F. Germano, G. Metelli, E. Giuriani, Experimental results on the role of sheathing-to-frame and base connections of a European timber framed shear wall, Construction and Building Materials, 80 (2015) 315–328.

[9] T. Vogt, J. Hummel, W. Seim, Timber framed wall elements under cyclic loading, Proceedings of the World Conference on Timber Engineering, 2012 WCTE, Auckland, 16-19 July.

[10] P. Grossi, T. Sartori, R. Tomasi, Tests on timber frame walls under in-plane forces: part 1, Proceedings of the Institution of Civil Engineers - Structures and Buildings 168, 11 (2015) 826-839

[11] N. Gattesco, A. Dudine, R. Franceschinis, Experimental investigation on the seismic behavior of timber shear walls with particle boards, 2012 WCTE, Auckland, 16-19 July.

[12] FEMA440 - Improvement of nonlinear static seismic analysis procedures, Federal Emergency Management Agency, 2005 June, Washington, D.C.

[13] S.A. Freeman, The Capacity Spectrum Method as a Tool for Seismic Design, 1998 ECEE, Paris, 6-11 September.

[14] M. Badoux, Comparison of Seismic Retrofitting Strategies with the Capacity Spectrum Method, 1998 ECEE, Paris, 6-11 September.